nature chemistry

Article

https://doi.org/10.1038/s41557-025-01734-x

Evolution of complex chemical mixtures reveals combinatorial compression and population synchronicity

Received: 3 November 2022

Accepted: 6 January 2025

Published online: 12 February 2025

Check for updates

Kavita Matange[1,2], Vahab Rajaei[1,2], Pau Capera-Aragones[1,2,3], John T. Costner[1,2], Adelaide Robertson[1,2], Jennifer Seoyoung Kim[1,2], Anton S. Petrov[1,2,4], Jessica C. Bowman[1,2,4], Loren Dean Williams[1,2,4] ✉ & Moran Frenkel-Pinter[1,3,5] ✉

Many open questions about the origins of life are centred on the generation of complex chemical species. Past work has characterized specific chemical reactions that might lead to biological molecules. Here we establish an experimental model of chemical evolution to investigate general processes by which chemical systems continuously change. We used water as a chemical reactant, product and medium. We leveraged oscillating water activity at near-ambient temperatures to cause ratcheting of near-equilibrium reactions in mixtures of organic molecules containing carboxylic acids, amines, thiols and hydroxyl groups. Our system (1) undergoes continuous change with transitions to new chemical spaces while not converging throughout the experiment; (2) demonstrates combinatorial compression with stringent chemical selection; and (3) displays synchronicity of molecular populations. Our results suggest that chemical evolution and selection can be observed in organic mixtures and might ultimately be adapted to produce a broad array of molecules with novel structures and functions.

Around four billion years ago, prebiotic chemistry established the molecular keystones of biology, paving a path to life[1,2]. Chemical and geological processes on the ancient Earth[3–5] increased the complexity of organic molecules, ultimately creating RNA, DNA, protein, polysaccharides and membrane-forming amphiphiles. Environmental energy was used in prebiotic formation of complex biopolymers, to establish the roots of biology. Prebiotic chemistry presents some of the most fascinating, important and difficult questions in the field of chemical sciences[6–14]. These questions centre on the nature of the chemistry that led to biology.

Some advances in our understanding of prebiotic chemistry come from systems chemistry[15–21], dynamic combinatorial chemistry (DCC)[22,23] and models of self-organization[24]. These approaches suggest that molecular heterogeneity of reactants promotes complex behaviours[15]. Dynamic combinatorial chemistry has achieved host–guest functionality[25,26], elaborate folds[27] and self-replication[28]. Mechanistic information has been revealed by mutually catalytic systems[14] and reproducing catalytic micelles[29]. Auto-catalytic production of macrocycles has been used for selecting molecules[20,21].

When subject to wet–dry cycling[30–32], certain chemical mixtures undergo striking changes in composition that seem relevant to the origins of life. Molecules can condense–dehydrate to form oligomers during the dry phase, and partially hydrolyse into smaller fragments during the wet phase. Glucose oligomerizes during wet–dry cycling to form oligosaccharides[33]; hydroxy acids oligomerize during wet–dry cycling to form polyesters[34–36]; and mixtures of hydroxy acids, mercapto acids and amino acids form oligomers that contain ester, thioester and amide bonds[11,37–45].

[1]NASA Center for Integration of the Origins of Life, Atlanta, GA, USA. [2]School of Chemistry and Biochemistry, Georgia Institute of Technology, Atlanta, GA, USA. [3]Institute of Chemistry, The Hebrew University of Jerusalem, Jerusalem, Israel. [4]NSF-NASA Center of Chemical Evolution, Atlanta, GA, USA. [5]The Center for Nanoscience and Nanotechnology, The Hebrew University of Jerusalem, Jerusalem, Israel. ✉e-mail: loren.williams@chemistry.gatech.edu; moran.fp@mail.huji.ac.il

https://doi.org/10.1038/s41557-025-01734-x

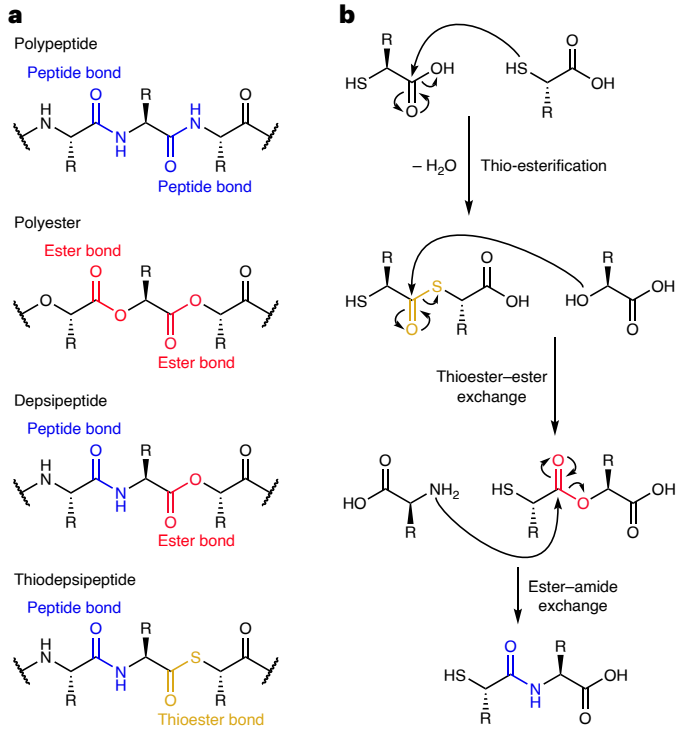

Fig. 1 | Peptide bonds are formed catalytically. a, The bond linkages via which polypeptides, polyesters, depsipeptides and thiodepsipeptides are formed. **b**, Progressive exploration of different chemical spaces during chemical evolution of mixtures containing hydroxy acids, mercapto acids and amino acids. Thioesters, formed by condensation–dehydration reactions between mercapto acids, are converted to esters by thioester–ester exchange with a hydroxy acid, which are then converted to amides via ester–amide exchange with an amino acid.

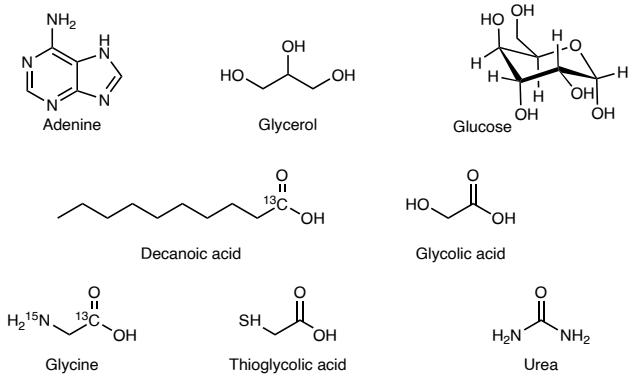

Fig. 2 | Nine chemical components were used to investigate chemical evolution. The MFP Set 3 components include adenine, glycerol, uniformly ^{13}C-labelled glucose, decanoic acid, glycolic acid, glycine, thioglycolic acid, urea and magnesium chloride (not shown).

Wet–dry cycling can build depsipeptides of select sequences[40] or amphiphiles composed of amino acid esters[46]. Cycling mixtures of amino and hydroxy acids, or diverse organic molecules, has resulted in emergence of function (hydrolase activity)[32,41]. Chemical spaces are progressively explored via wet–dry cycles: first, monomers are linked to form esters (or thioesters), which are then converted to amides via ester (or thioester) aminolysis (Fig. 1)[45,47].

A primary goal of our study here was to use wet–dry cycling to establish an experimental model of chemical evolution. Our experiments: (1) use water as the medium, and as a chemical reactant or a chemical product; (2) cycle water activity to oscillate driving forces; (3) use near-ambient temperatures; and (4) use complex mixtures of reactants that are 'connected', in that each molecule can react with all other molecules. Monomers condense into oligomers in the dry phase and partially hydrolyse in the wet phase. Products are selected first on condensation–dehydration chemistry, then on ester–amide exchange and then on resistance hydrolysis. Some products such as peptides are kinetically trapped and can persist as high-energy species during the wet phase. Environmental energy is converted to chemical energy. It is possible that such recursive processes contributed to the rise of biology from chemistry.

Our reactant mixtures are defined as complex if they contain diverse functional groups that can link via many chemical reactions to form very large numbers of products. Our initial mixture contains a hydroxy acid, an amino acid, a mercapto acid, urea, an aldohexose, a triol, an amphiphilic long-chain carboxylic acid, a purine and a hydrated divalent cation.

We observe novel outcomes from our experimental model. Our system continuously chemically transforms throughout the course of the experiment, does not combinatorially explode and demonstrates synchronized changes in populations of various chemical species. The results suggest that our model of chemical evolution can be extended and adapted to generate complex and useful molecules.

Results

The experimental platform

The primary focus of this report is the nine-component mixture (Fig. 2, MFP Set 3). However, experiments were performed with a variety of mixtures containing two-, three-, four-, five-, six-, nine- or 25-components. The mixtures are nested, in that subset mixtures omit reactants from parent reaction mixtures but do not include reactants not found in the parent mixture. Specifically, each two-, three-, four-, five- or six-component mixture is a subset of the nine-component mixture, which is a subset of the 25-component mixture.

Both single-step dry-down reactions and wet–dry cycling reactions were performed. Reactions were conducted under anoxic conditions at 45° C, with the exception of experiments investigating temperature dependence. Wet–dry cycling experiments took two days per cycle and were not fed with fresh reactants. Aliquots were taken after each cycle for C18–HPLC–UV–Vis, LC–MS and NMR analysis (Supplementary Figs. 1–44). The 15-cycle wet–dry cycling of the nine-component mixture was replicated five times (Supplementary Figs. 1 and 2). Chemical characterization is summarized in Supplementary Table 1. Sections of HPLC chromatograms are shown in Fig. 3. Single-step dry-down reactions, with similar mixtures, were conducted for three days. Figures 4 and 5, and Supplementary Figs. 6, 7 and 9 show HPLC chromatograms from single-step dry-down reactions.

Continuous chemical change

The realization of continuous change is indicated by inspection of chromatograms and by quantitation of rate of chemical change (Fig. 3c). We define chemical change by the net differences in concentrations between contiguous wet–dry cycles. The rate of change (R) is:

$$R = \frac{1}{N}\sum_{i=1}^{N}\frac{\left|P_i^{c+1} - P_i^{c}\right|}{\max\left(P_i^{c+1}, P_i^{c}\right)} \quad (1)$$

where N is the number of chemical species, and P_i^c is the concentration of species i at cycle c. The absolute value in equation (1) accounts for either increasing or decreasing concentration in an equal manner. The max() term in the denominator normalizes R such that it varies from 0 to 1, where 0 indicates no change and 1 represents complete transformation (maximal change detected). The concentration of each species is estimated by peak integral in HPLC chromatograms. This approximation does not account for differences in extinction coefficients. The experimental rate of change over 15 cycles—estimated from

https://doi.org/10.1038/s41557-025-01734-x

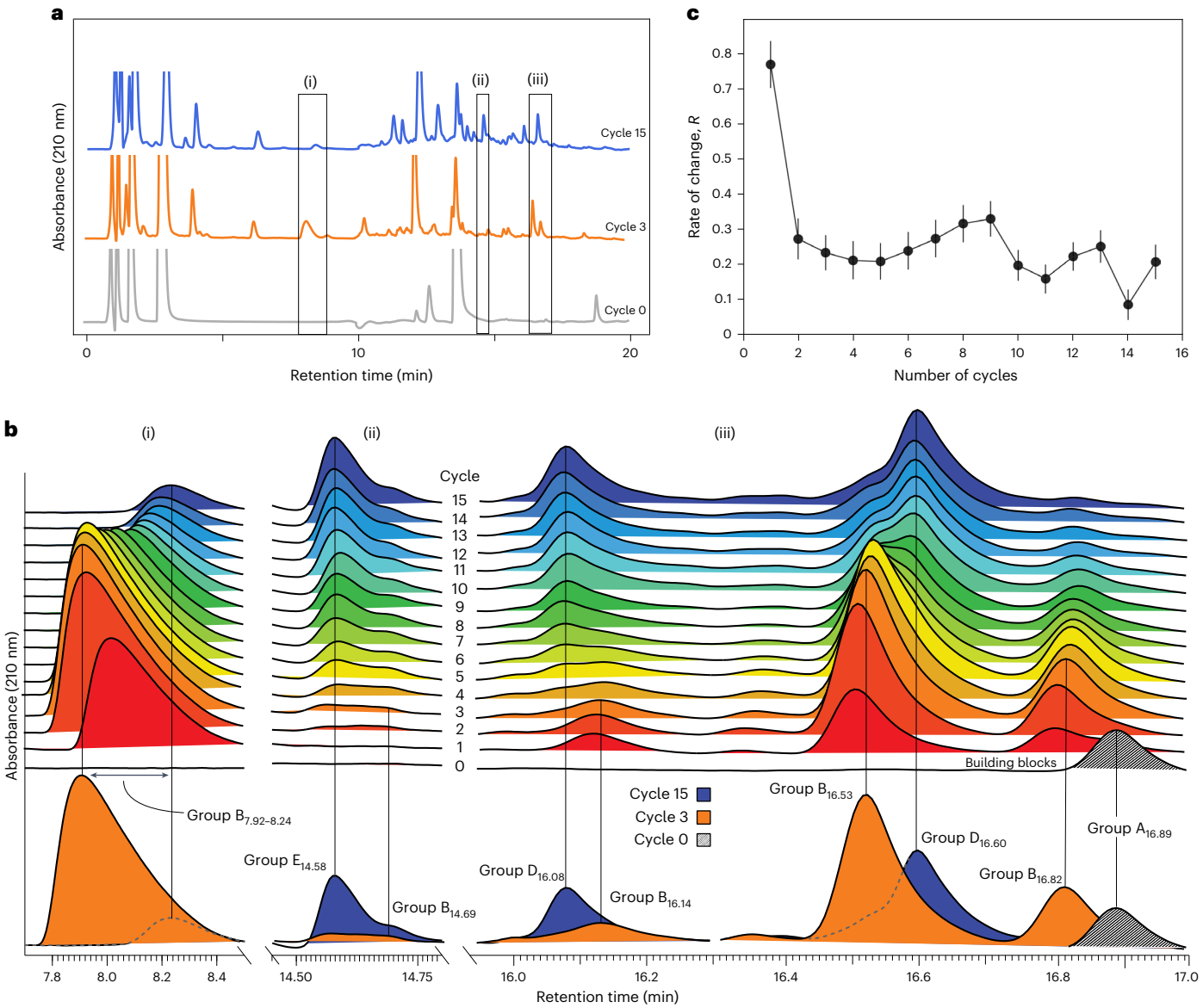

Fig. 3 | Chemical change is observed during wet–dry cycling. a, HPLC chromatograms of cycles 0, 3 and 15 of the nine-component mixture. Regions of chromatograms in boxes (i), (ii) and (iii) are enlarged in **b**. **b**, Top: an enlargement of select regions of the chromatogram showing all 15 cycles. Bottom: superimposition of common regions of the chromatograms of cycles 0, 3 and 15. Peaks partition into synchronous groups A, B, C, D or E by trajectory of population change. **c**, Rate of change (*R*) over 15 wet–dry cycles of the nine-component mixture at 210 nm. *R* is defined in equation (1), and is calculated using data from five independent replica experiments. Data are presented as mean values ± s.e.m.

equation (1)—is shown in Fig. 3c. The rate of change, *R*, was initially high and tended to a constant non-zero value after around five cycles. The system was evolving (changing) at an approximately constant rate from cycles 5 through 15. Although *R* remained relatively constant after cycle 5, the chemical composition of the system continuously changed during each of the 15 cycles. Every chromatogram is different from the flanking chromatograms. The system does not seem to converge after 15 cycles. The data show that the difference between cycles 14 and 15 was equivalent to differences between earlier pairs of contiguous cycles.

Combinatorial compression

Complex or even relatively simple mixtures undergoing chemical transformations tend to combinatorically explode[19,48–50]. Chemical reactants that can combine in multiple ways can form many products. The formose reaction, for example, produces a very large number of carbohydrate species[50,51].

In our experiments we were surprised to observe that the number of products (above the limit of detection) remains small and does not scale with the number of reactants. The number of products is not exponential—or even additive—with the number of reactants (Fig. 4). By contrast, a modest increase in temperature causes the number of products to explode (Fig. 5). We use the phrase 'combinatorial compression' to describe several interconnected phenomena. A combinatorially compressed reaction generates few product species from numerous diverse reactants. The number of product species does not increase with the number of reactants. Moreover, addition of reactants causes subtraction of products (Fig. 4); initiation of a reaction with the addition of new reactants leads to the formation of new products and the disappearance (subtraction) of other products.

More specifically, combinatorial compression was observed by comparing single-step dry-down reactions of a nine-component mixture with various two-, three-, four-, five- and six-component subsets of the nine-component mixture (Fig. 4a–c and Supplementary Fig. 6). For

https://doi.org/10.1038/s41557-025-01734-x

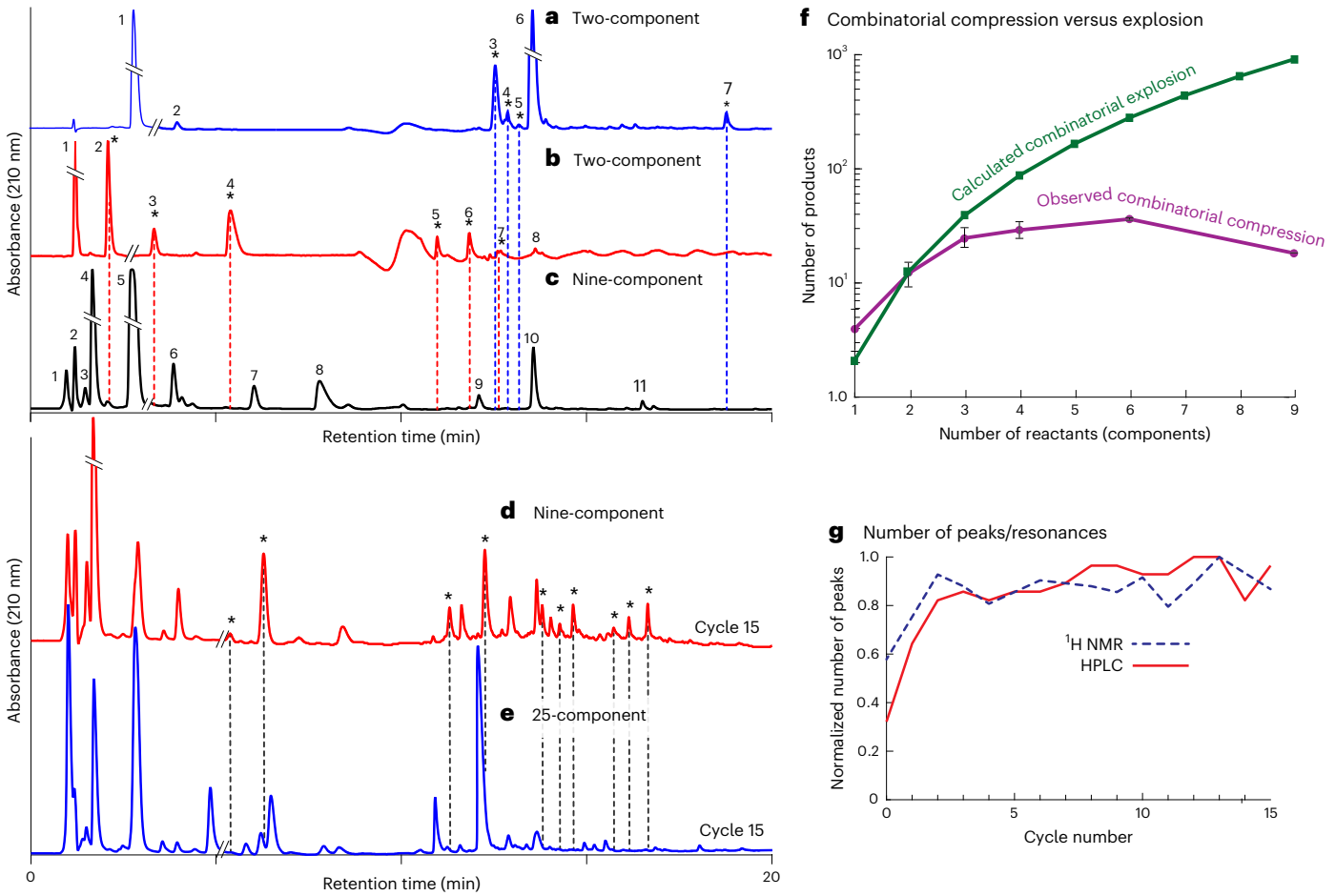

Fig. 4 | Combinatorial compression is observed at low temperature. **a**, A single-step dry-down reaction of a two-component mixture of thioglycolic acid and glucose reveals seven primary product peaks. **b**, A single-step dry-down of a two-component mixture of glycolic acid and glycerol reveals eight primary product peaks. **c**, A single-step dry-down reaction of a nine-component mixture that includes thioglycolic acid, glucose, glycolic acid and glycerol, plus additional components, results in only 11 primary product peaks. Asterisks indicate product peaks present in the two-component mixtures but absent from the nine-component mixture. All single-step dry-down reactions were conducted for 72 h. **d**, A chromatogram of the nine-component system after 15 wet–dry cycles. **e**, A chromatogram of the 25-component system after 15 wet–dry cycles. Asterisks indicate peaks present in the nine-component system but absent from the 25-component system. Product mixtures were separated using C18–HPLC. **f**, Observed and theoretical number of products from single-step dry-down reactions at 45 °C. Data are shown for one-, two-, three-, four-, six- and nine-component experiments. The theoretical number of products was calculated for length <4 (that is, only for dimers and trimers), assuming no branching, and with each permutation (that is, sequence) being distinct. The theoretical number of products is an underestimate because oligomers longer than trimers, and products formed by species reacting through more than two functional groups (possible for species such as glycerol and glucose), were not counted. We have made multiple independent measurements and report mean values ± s.e.m. **g**, Normalized peak counts in HPLC and ^{1}H NMR during wet–dry cycling of the nine-component system. The relative number of chemical species inferred by chromatography is consistent with the number of chemical species inferred by ^{1}H NMR.

example, the single-step dry-down of glucose and thioglycolic acid gave seven peaks (Fig. 4a), whereas the single-step dry-down of glycolic acid with glycerol gave eight peaks (Fig. 4b). This gives fifteen distinct peaks for these two different two-component reactions. The nine-component mixture—which contains all four of these components, plus an additional five components—gives only eleven primary peaks (Fig. 4c). Ten of the fifteen peaks observed in both of the two-component systems are absent (were subtracted) from the nine-component reaction. A comparison of these three reactions reveals the general phenomenon in which addition of reactants causes subtraction of products.

Combinatorial compression is also observed during wet–dry cycling. The nine-component MFP Set 3 mixture is a subset of the 25-component MFP Set 4 mixture. After 15 wet–dry cycles, many product peaks of the nine-component system are absent from the 25-component reaction (Fig. 4d,e). Ten of the 30 product peaks observed in cycle 15 of the nine-component system are absent from the 25-component mixtures, which contained 34 product peaks in total. Only 20 product peaks are shared between the two sets of reactions.

The balance between combinatorial compression and explosion is temperature dependent. Chromatograms of single-step dry-down reactions from three-, five- and nine-component systems from 25 °C to 85 °C are shown in Fig. 5. The results are dramatic. All three systems are compressed at low temperatures (≤45 °C) and the number of product peaks remains small in the three-, five- and nine-component systems. By contrast, high temperatures (≥55 °C) cause an explosion in the number of products in the systems, with the five- and nine-component systems showing broad peaks, consistent with a very large number of product species. The nine-component system has a broader peak than the five-component system, consistent with a greater diversity of product species.

Population synchronicity

We define population as the number of molecules of a chemical species; trajectory as the population change over wet–dry cycles; and

https://doi.org/10.1038/s41557-025-01734-x

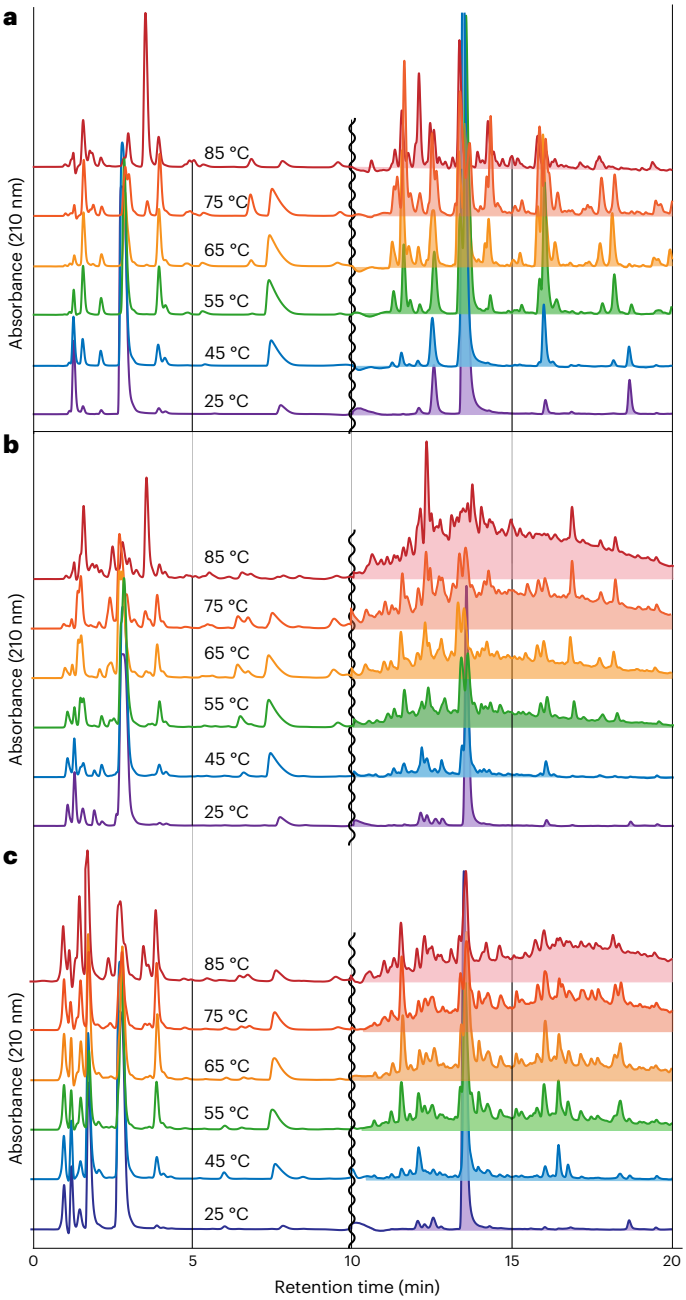

Fig. 5 | Combinatorial compression is observed at low temperatures while combinatorial explosion is observed at high temperatures. a–**c**, HPLC chromatograms of single-step dry-down reactions of three- (**a**), five- (**b**) and nine-component (**c**) systems. These nested mixtures were dried for three days under anoxic conditions over a range of temperatures. The HPLC chromatogram is displayed on a 1× scale from 0–10 min, and a 5× scale from 10–20 min. **a**, Three components: thioglycolic acid, glycolic acid and urea. **b**, Five components: thioglycolic acid, glycolic acid, urea, glycine and glucose. **c**, Nine-components (MFP Set 3). The number of peaks, as well as the broad peak seen at high temperature, signifies the formation of a large number of product species at high temperatures. The broad peak at high temperature moves to greater retention time (indicating more hydrophobic species) as the number of components increases. The peaks on the left—which elute before 5 min—are predominantly starting materials.

synchronicity as the similarity between trajectories of multiple species. We used a clustering algorithm[52,53] to partition trajectories into well-defined synchronous groups A–D (Fig. 6), and E (Supplementary Fig. 4). Group A's peaks correspond to starting components plus their immediate condensation products that form before the first dry-down cycle[44]. These peaks decrease rapidly during the early cycles. Group B's peaks sharply increase in population during cycles 1–3 and fall during cycles 4–15. Group C's peaks increase during cycles 1–5 and remain nearly constant during cycles 6–15. Group D's peaks form in cycle 3 and then steadily increase through cycle 15. Finally, group E's peaks remain nearly constant over 15 cycles. A dendrogram depicts hierarchical relationships within and between the groups (Fig. 6e).

Analysis of complex chemical systems

As discussed by Mamajanov and colleagues[19], complex chemical systems impose analytical challenges; however, extensive information regarding the nature of the products and their changes over cycles here was gathered by combining various analytical techniques such as LC–MS, HPLC, NMR and UV absorbance (Supplementary Table 1). The concordance of relative peak counts by ^{1}H NMR and HPLC (Fig. 4g) supports the utility of our peak-counting approach for quantitating the number of species. We observe that the number of peaks remains constant after cycle 3 but the chemical composition—as indicated by peak position and amplitude—does not. Our chromatography technique focused on hydrophobicity-based separation, in which resolution is poor for hydrophilic species. However, due to the chemical reactions anticipated (for example, the formation of thioester, ester and amide bonds), we expected that most of these product peaks will be well resolved in our analytical separation, an expectation that has been met based on peak shape and deconvolution analysis.

Some components of the nine-component system are more reactive than others. The nucleophilicity of sulfur is greater than that of oxygen, and thiols are better nucleophiles than hydroxyl groups. Accordingly, thioglycolic acid is more reactive than glycine[45]. These differences explain why initial products were observed that contained linkages to thioglycolic acid (peak with retention time of 8 min in Fig. 3b). By contrast, concentrations of unreactive species such as decanoic acid and adenine remained constant throughout the wet–dry cycling experiment (Supplementary Fig. 18).

Discussion

In this article we have established an experimental platform for studying and understanding chemical evolution based on wet–dry cycling. Our working definition of chemical evolution is continuous chemical change with exploration of new chemical spaces and avoidance of equilibrium. In our model, prebiotic chemical evolution is a specific example of a general phenomenon. In this work we have not prioritized prebiotic molecules as input and have not targeted biomolecules as output. Our intent was to enable continuous change without steering the system to preconceived molecular targets.

To explore wet–dry cycling, we used chemical species whose reactivity—in both thermodynamic and kinetic senses—is expected to be dependent on water activity. These species can covalently link and delink via reactions that release and absorb water, respectively. Component libraries used as inputs in our experiments are therefore connected in the sense that each member can in principle react with all others via functional groups such as hydroxyl groups, carboxylic acids, thiols and amines.

Using connected mixtures and low temperatures (≤45 °C), we have characterized reactions driven by wet–dry cycling. The results suggest that chemical systems can: (1) undergo continuous change while avoiding equilibrium; (2) exhibit combinatorial compression and population synchronicity; (3) transition to new chemical spaces, from monomers, to thioesters and esters, to amides; and (4) transduce environmental energy in kinetically trapped species. So far, continuous change in our experiments did not require feeding with fresh reactants; an initial ensemble of components underwent unceasing chemical change during environmental cycling throughout the course of the experiment.

We hypothesize that species that form readily but are resistant to hydrolysis by kinetic trapping can be selected via wet–dry cycling;

https://doi.org/10.1038/s41557-025-01734-x

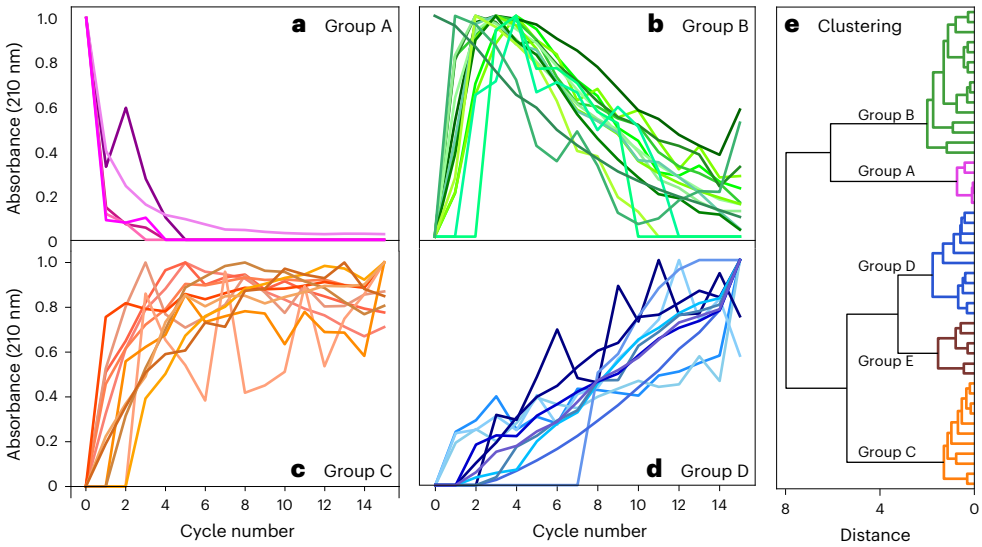

Fig. 6 | Synchronous changes in chemical populations are observed during wet–dry cycling. a, Group A molecules collapse in population during the early cycles. **b**, Group B molecules reach a maximum population near cycle 3 and fall over the next 12 cycles. **c**, Group C molecules increase in population during cycles 1 to 5 and thereafter remain constant. **d**, Group D molecules begin increasing in population at cycle 2 or 3 and increase until cycle 15. Group E molecules (not shown here; see Supplementary Fig. 4) show minimal change in population over cycles. **e**, Dendrograms depicting the hierarchical clustering of the changes in peak integrals over cycles. Data were obtained by fitting of modified Gaussians to HPLC chromatograms. Peak assignments are given in Supplementary Fig. 4 and Supplementary Table 1.

their populations increase over cycles. Thioesters and esters are readily made during the dry phase and hydrolyse readily during the wet phase (due to low activation energies). Amides are formed via ester or thioester intermediates during the dry phase, but are hydrolysed very slowly during the wet phase due to high activation energies. Wet–dry cycling can selectively grow populations of amides from esters or thioesters[38,43,45,54]. Although it has not been demonstrated here, we hypothesize that more prolonged cycling will select for molecules that fold, assemble and/or co-assemble. These phenomena confer additional resistance to hydrolysis[55] and contribute to increasingly deep kinetic traps. For example, assembled amphiphiles hydrolyse more slowly than isolated amphiphiles[56]; assembled peptides hydrolyse more slowly than free peptides[57,58]; and folded RNA hydrolyses more slowly than unfolded RNA[59].

Water is both the medium of biology and the chemical nexus of biochemistry[60]. Water is by far the most frequent and abundant chemical reagent in biology. Between one-third and one-half of known biochemical reactions involve chemical consumption or production of water, and all universal biopolymers and most metabolites are produced by condensation–dehydration reactions[60]. The centrality of water as both the medium and primary reactive species in biology is consistent with a model in which water governed chemical evolution during the origins of life. No other substance known to science can play such active roles as both a solvent with unique physical properties and as a hyperactive chemical reagent. During wet–dry cycling, water is a shared reactant, a shared product, and the reaction medium. Cycling water activity can cause reactions to oscillate in direction, and ratchet in energy and complexity.

Combinatorial compression

The mild temperatures of our reactions account, in part, for the differences in our results (compression) from many previous approaches (explosion). For complex mixtures at low temperatures, only a subset of many possible products is selected. For thermodynamically controlled reactions at 45 °C, a small difference of around 1.5 kcal mol^{-1} in reaction free energies ($\Delta\Delta G_{rxn}$) gives tenfold selectivity in equilibrium concentrations[61]. Similarly, for kinetically controlled reactions, a difference of around 1.5 kcal mol^{-1} in the activation free energies ($\Delta\Delta G^{\ddagger}$) gives tenfold selectivity in terms of reaction rates. For kinetically controlled reactions, the actual concentrations depend on the initial concentrations and reaction time. Selection of certain product species over others is based on these small differences in reaction free energies or activation energies. We have observed that the compression/explosion balance depends on temperature. The systems tip towards explosion as the temperature rises, whereas the systems tip towards compression as temperature decreases (Fig. 5).

Synchronicity

The system here displays synchronicity of trajectories where populations of groups of molecules rise and fall together over wet–dry cycles (Fig. 6). It will be of high interest in the future to apply mass balance calculations in a closed experimental system and track evolution of all chemical species.

Ratcheting

Wet–dry cycling causes oscillations between the linkage of components to form oligomers during the dried phase, and the partial depolymerization of oligomers into smaller fragments during the wet phase. Wet–dry cycling causes chemical ratcheting, where: a system advances towards an equilibrium state (but without reaching equilibrium); is redirected by the environmental cycle toward a different equilibrium state; and then is redirected again and again. Constant oscillations in the system seem sufficient to keep the system frustrated and prevent it from equilibrating. The system moves into progressively deeper kinetic traps. It is possible that such processes, continuing over a long period, contributed to the rise of biology.

Here we assume that chemistry is continuous with biology and use that continuity to inform our working model of chemical evolution based on wet–dry cycling. This model maps evolutionary concepts onto chemical processes. In this model, we say that: (1) a generation is a single wet–dry cycle; (2) heredity is information passed from one generation to the next; (3) information is associated with non-random chemical composition; (4) selection results in inheritance of certain molecular species over generations; (5) fitness confers persistence (that is, survival) of molecules and specific molecular assemblies; and (6) water is an energy currency that links reactions and, upon changing activity, alters reaction free energies.

Future prospects

As noted by François Jacob: "the really creative part in biochemistry must have occurred very early"[62]. Biopolymers are some of nature's most creative accomplishments. We do not yet know if wet–dry cycling can create proto-biological structures and functions. What happens after 150 cycles or 15,000 cycles? What happens if we feed the system? What happens if we switch less reactive components to more reactive analogues, increase chemical diversity of the reactants, or change their concentration, or the cycling frequency? In the next series of experiments, currently in progress, these issues will be explored.

Online content

Any methods, additional references, Nature Portfolio reporting summaries, source data, extended data, supplementary information, acknowledgements, peer review information; details of author contributions and competing interests; and statements of data and code availability are available at https://doi.org/10.1038/s41557-025-01734-x.

References

1. Bell, E. A., Boehnke, P., Harrison, T. M. & Mao, W. L. Potentially biogenic carbon preserved in a 4.1 billion-year-old zircon. *Proc. Natl Acad. Sci. USA* **112**, 14518–14521 (2015).
2. Orgel, L. E. The origin of life on the earth. *Sci. Am.* **271**, 76–83 (1994).
3. Trainer, M. G. et al. Organic haze on Titan and the early Earth. *Proc. Natl Acad. Sci. USA* **103**, 18035–18042 (2006).
4. Reed, N. W., Wing, B. A., Tolbert, M. A. & Browne, E. C. Trace H_2S promotes organic aerosol production and organosulfur compound formation in archean analog haze photochemistry experiments. *Geophys. Res. Lett.* **49**, e2021GL097032 (2022).
5. Zahnle, K. J., Lupu, R., Catling, D. C. & Wogan, N. Creation and evolution of impact-generated reduced atmospheres of early Earth. *Planetary Sci. J.* **1**, 11 (2020).
6. Hud, N. V., Cafferty, B. J., Krishnamurthy, R. & Williams, L. D. The origin of RNA and 'my grandfather's axe'. *Chem. Biol.* **20**, 466–474 (2013).
7. Brack, A. Selective emergence and survival of early polypeptides in water. *Orig. Life Evol. Biosph.* **17**, 367–379 (1987).
8. Schneider, C. et al. Noncanonical RNA nucleosides as molecular fossils of an early Earth—generation by prebiotic methylations and carbamoylations. *Angew. Chem. Int. Ed.* **57**, 5943–5946 (2018).
9. Deamer, D. The role of lipid membranes in life's origin. *Life* **7**, 5 (2017).
10. Kim, S. C. et al. A model for the emergence of RNA from a prebiotically plausible mixture of ribonucleotides, arabinonucleotides, and 2′-deoxynucleotides. *J. Am. Chem. Soc.* **142**, 2317–2326 (2020).
11. Frenkel-Pinter, M. et al. Selective incorporation of proteinaceous over nonproteinaceous cationic amino acids in model prebiotic oligomerization reactions. *Proc. Natl Acad. Sci. USA* **116**, 16338–16346 (2019).
12. Runnels, C. M. et al. Folding, assembly, and persistence: the essential nature and origins of biopolymers. *J. Mol. Evol.* **86**, 598–610 (2018).
13. Cleaves II, H. J. The origin of the biologically coded amino acids. *J. Theor. Biol.* **263**, 490–498 (2010).
14. Vincent, L. et al. Chemical ecosystem selection on mineral surfaces reveals long-term dynamics consistent with the spontaneous emergence of mutual catalysis. *Life* **9**, 80 (2019).
15. Cafferty, B. J. et al. Robustness, entrainment, and hybridization in dissipative molecular networks, and the origin of life. *J. Am. Chem. Soc.* **141**, 8289–8295 (2019).
16. Segré, D., Ben-Eli, D. & Lancet, D. Compositional genomes: prebiotic information transfer in mutually catalytic noncovalent assemblies. *Proc. Natl Acad. Sci. USA* **97**, 4112–4117 (2000).
17. Kroiss, D., Ashkenasy, G., Braunschweig, A. B., Tuttle, T. & Ulijn, R. V. Catalyst: can systems chemistry unravel the mysteries of the chemical origins of life? *Chem* **5**, 1917–1920 (2019).
18. Ashkenasy, G., Hermans, T. M., Otto, S. & Taylor, A. F. Systems chemistry. *Chem. Soc. Rev.* **46**, 2543–2554 (2017).
19. Guttenberg, N., Virgo, N., Chandru, K., Scharf, C. & Mamajanov, I. Bulk measurements of messy chemistries are needed for a theory of the origins of life. *Philos. Trans. R. Soc. A* **375**, 20160347 (2017).
20. Wołos, A. et al. Synthetic connectivity, emergence, and self-regeneration in the network of prebiotic chemistry. *Science* **369**, eaaw1955 (2020).
21. Miao, X. et al. Kinetic selection in the out-of-equilibrium autocatalytic reaction networks that produce macrocyclic peptides. *Angew. Chem. Int. Ed.* **133**, 20529–20538 (2021).
22. Cao, Y. et al. Self-synthesizing nanorods from dynamic combinatorial libraries against drug resistant cancer. *Angew. Chem. Int. Ed.* **133**, 3099–3107 (2021).
23. Komáromy, D., Nowak, P. & Otto, S. in *Dynamic Covalent Chemistry: Principles, Reactions, and Applications* 31–119 (Wiley, 2017).
24. Chvykov, P. et al. Low rattling: a predictive principle for self-organization in active collectives. *Science* **371**, 90–95 (2021).
25. Otto, S., Furlan, R. L. & Sanders, J. K. Selection and amplification of hosts from dynamic combinatorial libraries of macrocyclic disulfides. *Science* **297**, 590–593 (2002).
26. Lam, R. T. et al. Amplification of acetylcholine-binding catenanes from dynamic combinatorial libraries. *Science* **308**, 667–669 (2005).
27. Liu, B. et al. Complex molecules that fold like proteins can emerge spontaneously. *J. Am. Chem. Soc.* **141**, 1685–1689 (2018).
28. Carnall, J. M. et al. Mechanosensitive self-replication driven by self-organization. *Science* **327**, 1502–1506 (2010).
29. Kahana, A. & Lancet, D. Self-reproducing catalytic micelles as nanoscopic protocell precursors. *Nat. Rev. Chem.* **5**, 870–878 (2021).
30. Mamajanov, I. et al. Ester formation and hydrolysis during wet–dry cycles: generation of far-from-equilibrium polymers in a model prebiotic reaction. *Macromolecules* **47**, 1334–1343 (2014).
31. Damer, B. & Deamer, D. The hot spring hypothesis for an origin of life. *Astrobiology* **20**, 429–452 (2020).
32. Foster, K., Hillman, B., Rajaei, V., Seng, K. & Maurer, S. Evolution of realistic organic mixtures for the origins of life through wet–dry cycling. *Sci* **4**, 22 (2022).
33. Li, Z. et al. The oligomerization of glucose under plausible prebiotic conditions. *Orig. Life Evol. Biosph.* **49**, 225–240 (2019).
34. Jia, T. Z. et al. Incorporation of basic α-hydroxy acid residues into primitive polyester microdroplets for RNA segregation. *Biomacromolecules* **22**, 1484–1493 (2021).
35. Jia, T. Z. & Chandru, K. Recent progress in primitive polyester synthesis and membraneless microdroplet assembly. *Biophys. Physicobiol.* **20**, e200012 (2023).
36. Jia, T. Z. et al. Membraneless polyester microdroplets as primordial compartments at the origins of life. *Proc. Natl Acad. Sci. USA* **116**, 15830–15835 (2019).
37. Rodriguez-Garcia, M. et al. Formation of oligopeptides in high yield under simple programmable conditions. *Nat. Commun.* **6**, 8385 (2015).
38. Forsythe, J. G. et al. Ester-mediated amide bond formation driven by wet–dry cycles: a possible path to polypeptides on the prebiotic earth. *Angew. Chem. Int. Ed.* **54**, 9871–9875 (2015).
39. Yu, S. et al. Elongation of model prebiotic proto-peptides by continuous monomer feeding. *Macromolecules* **50**, 9286–9294 (2017).
40. Forsythe, J. G. et al. Surveying the sequence diversity of model prebiotic peptides by mass spectrometry. *Proc. Natl Acad. Sci. USA* **114**, E7652–E7659 (2017).

41. Doran, D., Abul-Haija, Y. M. & Cronin, L. Emergence of function and selection from recursively programmed polymerisation reactions in mineral environments. *Angew. Chem. Int. Ed.* **58**, 11253–11256 (2019).
42. Bouza, M. et al. Compositional characterization of complex protopeptide libraries via triboelectric nanogenerator orbitrap mass spectrometry. *Rapid Commun. Mass Spectr.* **33**, 1293–1300 (2019).
43. Frenkel-Pinter, M. et al. Mutually stabilizing interactions between proto-peptides and RNA. *Nat. Commun.* **11**, 3137 (2020).
44. Frenkel-Pinter, M., Sargon, A. B., Glass, J. B., Hud, N. V. & Williams, L. D. Transition metals enhance prebiotic depsipeptide oligomerization reactions involving histidine. *RSC Adv.* **11**, 3534–3538 (2021).
45. Frenkel-Pinter, M. et al. Thioesters provide a plausible prebiotic path to proto-peptides. *Nat. Commun.* **13**, 2569 (2022).
46. Lago, I., Black, L., Wilfinger, M. & Maurer, S. E. Synthesis and characterization of amino acid decyl esters as early membranes for the origins of life. *Membranes* **12**, 858 (2022).
47. Frenkel-Pinter, M., Samanta, M., Ashkenasy, G. & Leman, L. J. Prebiotic peptides: molecular hubs in the origin of life. *Chem. Rev.* **120**, 4707–4765 (2020).
48. Asche, S., Cooper, G. J. T., Keenan, G., Mathis, C. & Cronin, L. A robotic prebiotic chemist probes long-term reactions of complexifying mixtures. *Nat. Commun.* **12**, 3547 (2021).
49. Marshall, S. M. et al. Identifying molecules as biosignatures with assembly theory and mass spectrometry. *Nat. Commun.* **12**, 3033 (2021).
50. Orgel, L. E. Prebiotic chemistry and the origin of the RNA world. *Crit. Rev. Biochem. Mol. Biol.* **39**, 99–123 (2004).
51. Colón-Santos, S., Cooper, G. J. & Cronin, L. Taming combinatorial explosion of the formose reaction via recursion within mineral environments. *ChemSystemsChem* **1**, e1900014 (2019).
52. van Duppen, P., Daines, E., Robinson, W. E. & Huck, W. T. Dynamic environmental conditions affect the composition of a model prebiotic reaction network. *J. Am. Chem. Soc.* **145**, 7559–7568 (2023).
53. Virtanen, P. et al. SciPy 1.0: fundamental algorithms for scientific computing in Python. *Nat. Methods* **17**, 261–272 (2020).
54. Yu, S. S. et al. Kinetics of prebiotic depsipeptide formation from the ester-amide exchange reaction. *Phys. Chem. Chem. Phys.* **18**, 28441–28450 (2016).
55. Edri, R., Fisher, S., Menor-Salvan, C., Williams, L. D. & Frenkel-Pinter, M. Assembly-driven protection from hydrolysis as key selective force during chemical evolution. *FEBS Lett.* **597**, 2879–2896 (2023).
56. Kensil, C. R. & Dennis, E. A. Alkaline hydrolysis of phospholipids in model membranes and the dependence on their state of aggregation. *Biochemistry* **20**, 6079–6085 (1981).
57. Abkevich, V. I., Gutin, A. M. & Shakhnovich, E. I. How the first biopolymers could have evolved. *Proc. Natl Acad. Sci. USA* **93**, 839–844 (1996).
58. Prusiner, S. B. Prions. *Proc. Natl Acad. Sci. USA* **95**, 13363–13383 (1998).
59. Nahvi, A. et al. Genetic control by a metabolite binding mRNA. *Chem. Biol.* **9**, 1043–1049 (2002).
60. Frenkel-Pinter, M., Rajaei, V., Glass, J. B., Hud, N. V. & Williams, L. D. Water and life: the medium is the message. *J. Mol. Evol.* **89**, 2–11 (2021).
61. Lowry, T. & Richardson, K. *Mechanism and Theory in Organic Chemistry* (Harper & Row, 1981).
62. Jacob, F. Evolution and tinkering. *Science* **196**, 1161–1166 (1977).

Data availability

The data supporting the findings of this study are available within the article and its Supplementary Information.

Code availability

Our Python code for calculating continuous chemical change—which corrects the chromatogram baseline, and identifies and integrates peaks—is available at: https://github.com/HUJI-MFP/HPLC_automatic_analysis/blob/main/HPLC_python.py.

Acknowledgements

We thank N. Hud, M.G. Finn, G. Schuster, M. Grover, M. Travisano, D. Lancet and E. Smith for helpful comments. Funding: This research was supported by the National Science Foundation (grant no. 1724274 to L.D.W.), NASA Center for Integration of the Origins of Life (grant no. 80NSSC24K0344), the Azrieli Foundation Early Career Faculty Grant (to M.F.P.), the Israel Science Foundation grant (grant no. 1611/22 to M.F.P.), the Minerva Foundation (to M.F.P.) and FEBS Foundation Excellence Award (to M.F.P.).

Author contributions

M.F.P. and K.M. performed dry-down and wet–dry cycling experiments. M.P.F., K.M. and V.R. performed chemical analysis. K.M., A.R., J.S.K. and M.F.P. performed analysis of HPLC data. P.C.A. wrote a Python code for automatic analysis of HPLC data. V.R. performed the NMR analysis. A.S.P. and J.T.C. performed analysis of MS data. M.F.P., K.M. and L.D.W. formulated models, and conceived and designed experiments. M.F.P., K.M., V.R., J.C.B., P.C.A. and L.D.W. wrote the paper.

Competing interests

The authors declare no competing interests.

Additional information

Supplementary information The online version contains supplementary material available at https://doi.org/10.1038/s41557-025-01734-x.

Correspondence and requests for materials should be addressed to Loren Dean Williams or Moran Frenkel-Pinter.

Peer review information *Nature Chemistry* thanks David Baum, Shawn McGlynn and the other, anonymous, reviewer(s) for their contribution to the peer review of this work.